Crystal structure and size distribution of Pt–Cu–Fe alloy clusters supported on carbon black

Whanjin Roh, Jihoon Cho and Hasuck Kim

Department of Chemistry and Center for Molecular Catalysis, Seoul National University, San 56-1, Shinrim-dong, Kwanak-ku, Seoul 151-742, Korea

Received 20 March 1995; accepted 10 November 1995

Carbon supported alloy electrocatalysts based on Pt, Cu and Fe (atomic ratios Pt : Cu : Fe = 2 : 1 : 1 and 6 : 1 : 1) are prepared at various alloying temperatures and are characterized by XRD and TEM techniques. Powder XRD analyses show that Pt_6CuFe clusters form a face-centered cubic structure ($AuCu_3$ type), while Pt_2CuFe clusters form an ordered alloy with a face-centered tetragonal structure (AuCu type) at higher temperature than 700°C. Transmission electron micrographs reveal that the size of metal clusters increases gradually and size distribution becomes broader, as alloying temperature increases from 500 to 1100°C.

Keywords: fuel cell; supported electrocatalysts; X-ray diffraction; electron microscopy; alloy structure

1. Introduction

In low temperature fuel cells, the high overpotential for oxygen reduction slows down the commercialization of these technologies. Thus, many investigators are devoted to developing new electrocatalysts to improve oxygen reduction rate. Platinum supported on carbon black has been used for many years for oxygen reduction reaction in phosphoric acid fuel cell mainly owing to its long term stability, even though it has cost disadvantage.

In the patent area [1–5], it has recently been reported that alloying supported Pt with one or more transition metals such as V, Cr, Co, Fe, Cu, etc., has improved the electrochemical activity for oxygen reduction. To elucidate the alloying effect, several investigators have studied binary alloys such as Pt–Cr [6], Pt–Ti [7], Pt–Co [8], and Pt–Fe [9]. Srinivasan et al. [10] reported that the enhanced electrocatalytic activity exhibited by binary Pt alloys appeared to originate primarily as a result of changes in the lattice structure owing to alloying. But there still remains debate on the reason for the increased activity and exact characterization of those supported alloy catalysts is needed.

In the present work, we report on the preparation of carbon black supported Pt–Cu–Fe ternary alloy electrocatalysts with two atomic compositions, Pt : Cu : Fe = 6 : 1 : 1 and 2 : 1 : 1, which show enhanced activity for the reduction of oxygen in phosphoric acid fuel cell. We also report on the change of crystal structure and size distribution of supported metal clusters with heat-treatment temperatures by X-ray diffraction (XRD) and transmission electron microscope (TEM) techniques.

2. Experimental

Alloy catalysts were prepared starting from a commercially available Pt catalyst supported on Vulcan XC-72R (Johnson Matthey, 10 wt% Pt, about 120 m^2/g Pt). One gram of Pt/C was dispersed into 25 ml of deionized water and ultrasonically blended for 10 min. Appropriate amounts of 0.1 M solution of transition metal salts ($FeCl_2$, $CuCl_2$) were added to this suspension respectively. The atomic ratio of Pt, Cu and Fe was adjusted either to 6 : 1 : 1 (series A) or 2 : 1 : 1 (series B) in all resulting catalysts. Then the pH of the solution was adjusted to 8 by dropwise addition of 0.5 M NH_4OH. After ultrasonic blending for 20 min and further stirring for 5 h, the suspension was filtered with a very dense filter paper and the residue was dried at 100°C for 2 h. The quantitative amount of the loaded metal was determined with an inductively coupled plasma–atomic emission spectroscope (ICP-AES, Labtam). The dried catalysts were heat-treated at 500, 700, 900, and 1100°C for 2.5 h respectively in reducing atmosphere (10% H_2 and 90% N_2) for reduction and alloying, and then cooled to room temperature under flowing inert gas.

Powder X-ray diffraction patterns of these supported catalysts were obtained with a Rigaku CN2115 diffractometer with nickel-filtered Cu Kα radiation. The X-ray gun was operated at 40 kV and 30 mA and at a scanning rate of 5°/min (2 theta). Powder samples were mounted on glass slides.

For the TEM observation, a few catalysts were ultrasonically dispersed in methanol, and gathered on a carbon-coated copper grid. Bright field micrographs were

obtained using a Jeol-200CX at an accelerating voltage of 160 kV.

3. Results and discussion

3.1. X-ray diffraction

Powder X-ray diffraction technique was applied to determine the crystal lattice structure of supported metal clusters, the extent of order–disorder transformation, and to estimate the size of metal clusters.

Fig. 1 shows the XRD patterns of series A catalysts (Pt : Cu : Fe = 6 : 1 : 1), and supported unalloyed Pt catalyst for comparison. Pt clusters exhibit a face-centered cubic lattice structure like that of bulk Pt metal. As the heat-treatment temperature increases, diffraction peaks become narrower and clearer because the particle size grows by sintering and thus the lattice crystal structure is apparent.

At the heat-treatment temperature of 500°C, the alloy clusters form a disordered alloy as Cu or Fe interpenetrates randomly into a lattice of Pt atoms, as shown in fig. 2a. Also it can be seen that the trace of new peaks appears and becomes apparent above 700°C. These extra peaks are called superlattice lines [11], and their presence is direct evidence that an ordered alloy has formed, in which Cu or Fe atoms have displaced particular Pt atomic sites, as shown in fig. 2b. Fig. 3 shows XRD patterns of series B catalysts (Pt : Cu : Fe = 2 : 1 : 1). Contrary to series A, the crystal structure of alloyed clusters is transformed into a tetragonal lattice structure like mineral tulameenite [12], which is confirmed distinctively by splitting of the (220) and (200) diffraction peaks to (220), (202) and (200), (002) peaks respectively.

The results of XRD analysis are summarized in table 1. The lattice parameter is calculated by least squares linear extrapolation from (111), (200), (220), (202), and (311) peaks. As heat-treatment temperature increases, the lattice parameter of series A catalysts changes gradually from the unalloyed Pt value of $a = 3.924$ Å to the heat-treated (1100°C) catalyst value of 3.851 Å. Upon alloy formation with smaller atoms

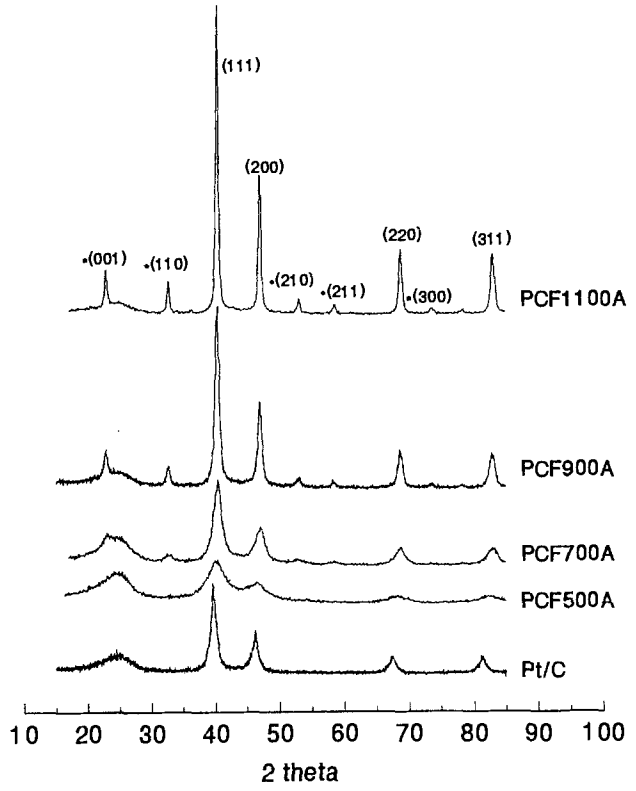

Fig. 1. XRD patterns of series A catalysts (Pt : Cu : Fe = 6 : 1 : 1) and unalloyed Pt catalyst (Pt/C). Each sample is denoted as PCF and followed by heat-treated temperature. Superlattice peaks are indicated by *. Pt/C is heat-treated at 900°C.

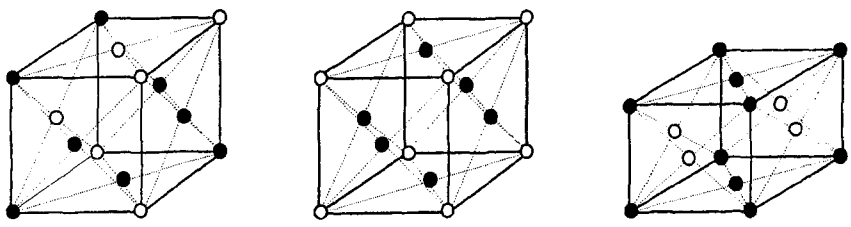

(a) disordered alloy face-centered cubic structure

(b) Pt_6CuFe ordered alloy face-centered cubic structure

(c) Pt_2CuFe ordered alloy face-centered tetragonal structure

● Platinum atoms ○ Cu or Fe atoms

Fig. 2. The lattice structure of unit cell of Pt–Cu–Fe alloy catalysts.

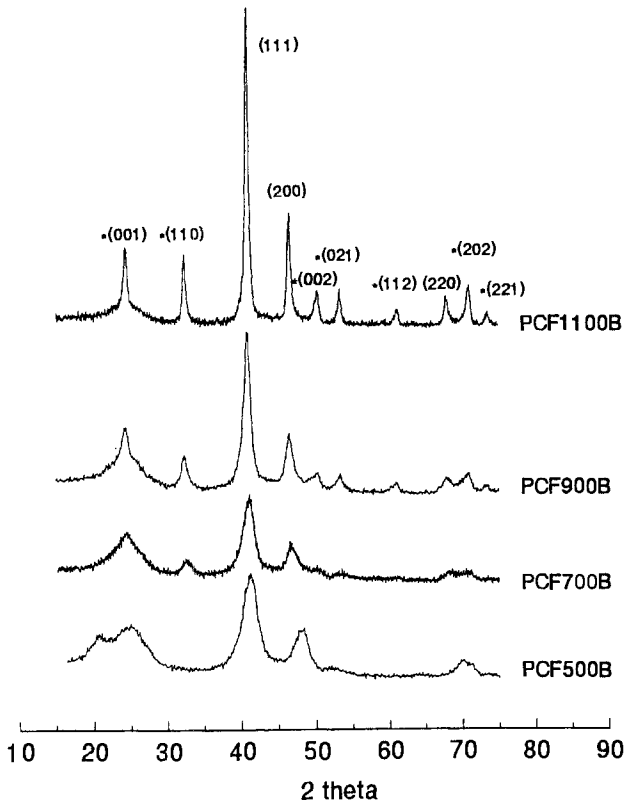

Fig. 3. XRD patterns of series B catalysts (Pt : Cu : Fe = 2 : 1 : 1).

like Cu or Fe, the lattice structure of Pt has contracted. Contrary to series A, the series B catalysts show different tendency. The sample of heat-treated catalyst at 500°C has the lattice parameter of 3.926 Å which is almost the same as that of unalloyed Pt. But from 700°C, the cubic cell undergoes a slight tetragonal distortion (c/a = 0.945–0.929), because smaller Cu or Fe atoms segregate into designated sites. As shown in fig. 2c, Pt atoms occupy (0, 0, 0) and (1/2, 1/2, 0) positions, while Cu or Fe atoms occupy (1/2, 0, 1/2) and (0, 1/2, 1/2) lattice points [13]. The distortion extends further with increased heat-treatment temperature.

The relative intensity of the (110) superlattice line to the (111) fundamental line indicates the extent of ordered alloy formation [11]. As the heat-treatment temperature increases, the peak area ratio of (110) to (111) increases in both series A and B on the whole. But there is almost no change in those of the catalysts heat-treated at 900 and 1100°C, which indicates that the formation of ordered alloy has completed at 900°C. Thus, heat-treatment at higher temperature than 900°C only results in the reduction of metal dispersion.

The average size of supported metal clusters is calculated with the line width of the (111) diffraction line using Scherrer's formula [14]. The instrumental broadening is corrected using the peak broadening from silicon powder whose particle size is large enough to eliminate any particle size broadening effect. The cluster size increases gradually with increasing temperature, as shown in the last column of table 1. Especially, large clusters reaching to about 200 Å are produced in the heat-treated catalyst at 1100°C.

3.2. TEM analysis

The morphology of supported metal clusters is observed by TEM. Fig. 4 shows TEM images for series A catalysts that have good contrast between spherical metal phase and agglomerates of carbon black supports. Metal clusters are well dispersed on carbon black support in catalyst samples heat-treated at 500 and 700°C. As expected, the size of metal clusters increases and therefore, it results in reduced dispersion depending on the heat-treatment temperature. Above 900°C, abnor-

Table 1
Results of XRD and TEM analysis for Pt–Cu–Fe/C catalysts

Catalyst	Lattice structure	Lattice parameter (Å)			(110)/(111) peak ratio (%)	Particle size (Å)	
		a	c	c/a		XRD	TEM
PCF500A[a]	fcc[d]	3.873			0	34.6	35.1
PCF700A	fcc	3.860			7.9	59.9	56.5
PCF900A	fcc	3.861			11.2	123	104
PCF1100A	fcc	3.851			9.6	205	156
PCF500B[b]	fcc	3.926			0	35.9	33.0
PCF700B	fct[e]	3.897	3.684	0.945	14.1	53.2	53.1
PCF900B	fct	3.891	3.621	0.931	21.2	79.5	87.8
PCF1100B	fct	3.903	3.625	0.929	23.2	178	151
Pt/C[c]	fcc	3.924				41.6	

[a] Series A catalyst (Pt : Cu : Fe = 6 : 1 : 1) with heat-treatment at 500°C.
[b] Series B catalyst (Pt : Cu : Fe = 2 : 1 : 1) with heat-treatment at 500°C.
[c] Unalloyed Pt catalyst heat-treated at 900°C.
[d] fcc: face-centered cubic.
[e] fct: face-centered tetragonal.

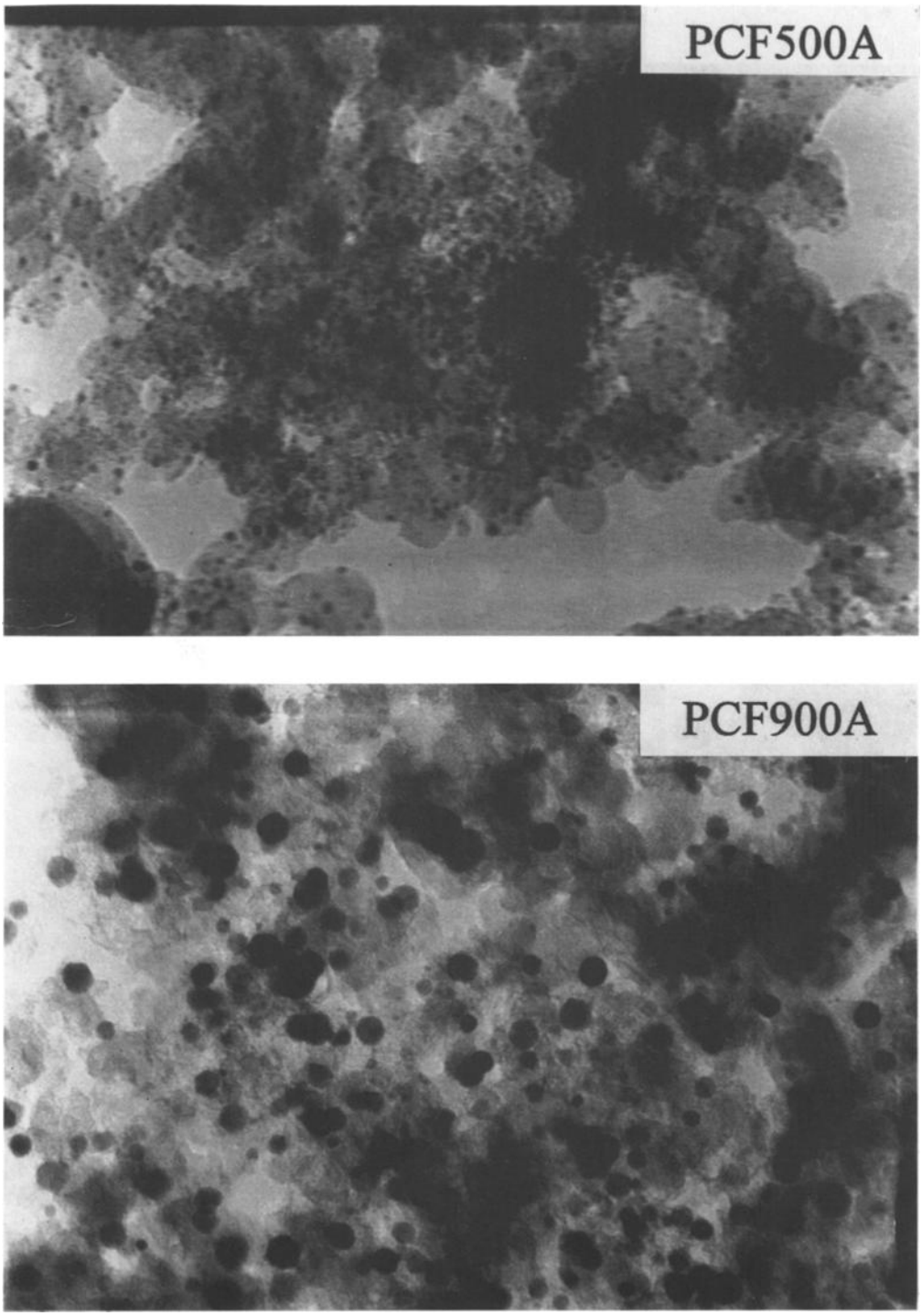

Fig. 4. TEM micrographs of series A catalysts. Series B catalysts showed similar tendency. (X 200 000)

mally large clusters are produced and thus, metal clusters are sparsely distributed.

Fig. 5 summarizes the statistical results from examining about 200–300 particles in three different parts of each catalyst sample. The size distribution of heat-treated catalyst at 500°C exhibits a narrow distribution with an average size of 35 Å. As the heat-treatment temperature increases, the average cluster size is displaced to a larger part, abnormally small particles disappear, and larger particles start to appear. Thereby, the range of particle size distribution becomes wide. The mean size of clusters evaluated by TEM is compared with that of the

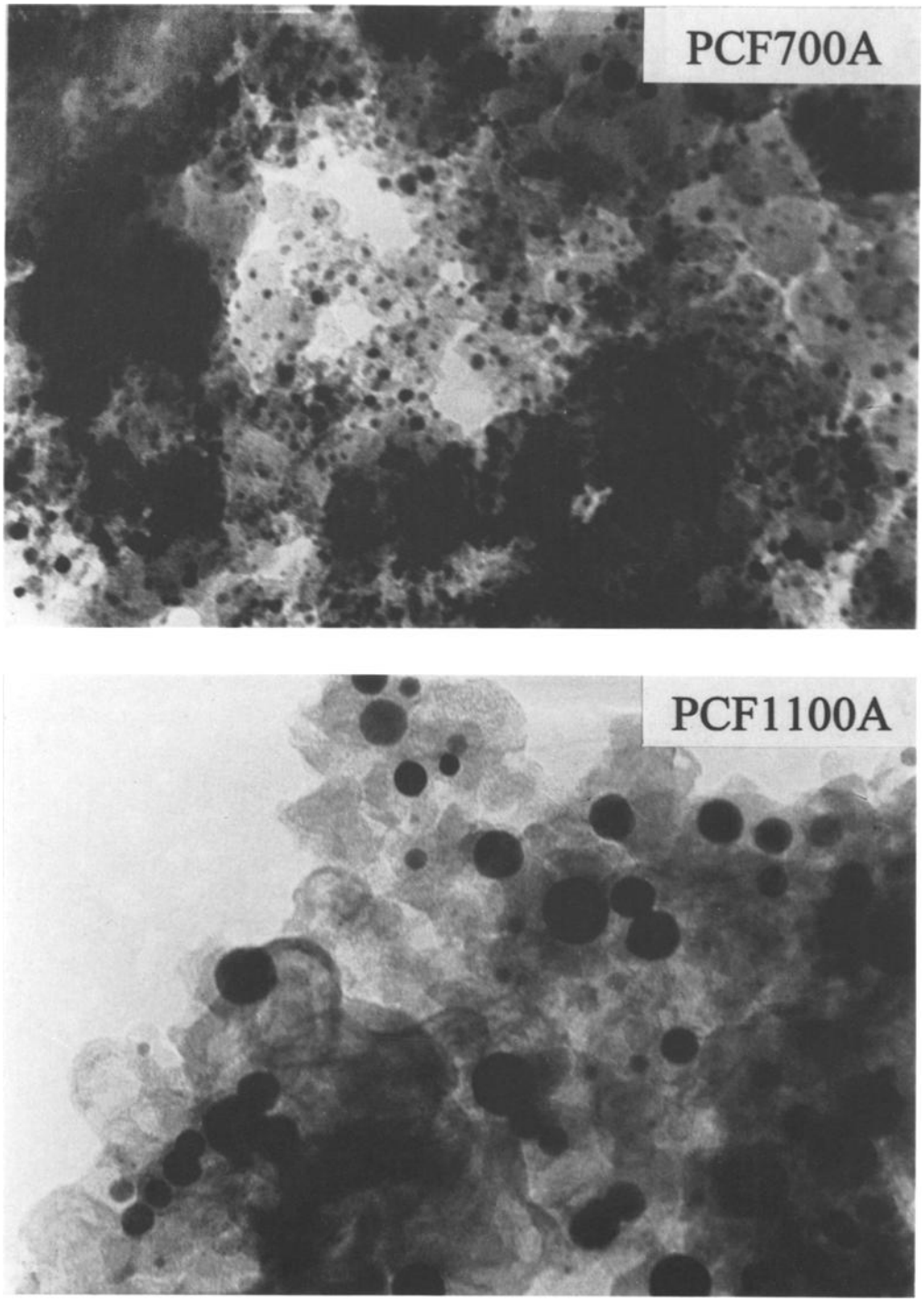

Fig. 4. (Continued).

XRD method in table 1. The two techniques agree well in 500 and 700°C heat-treated catalysts that have narrow size distribution. But in the case of broader size distributions (900 and 1100°C samples), XRD line broadening is not accurate for the determination of the average cluster size. This is probably due to the fact that XRD is a volume averaging technique that results in an overestimate of one dimensional size.

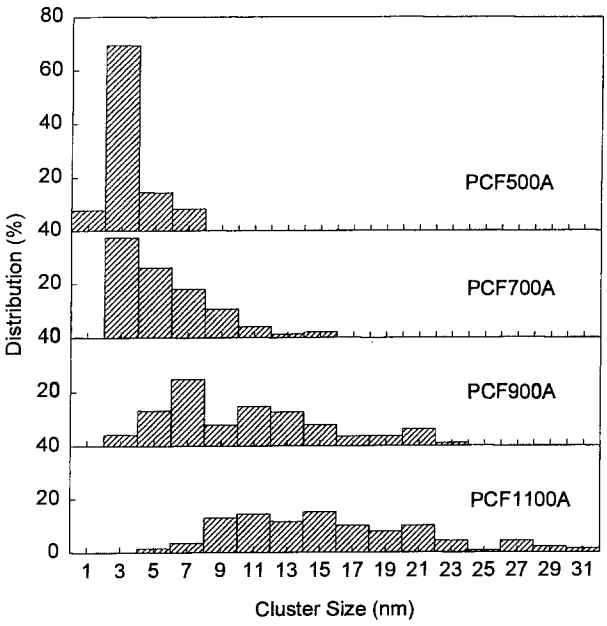

Fig. 5. Size distribution of alloy clusters in series A catalysts. Series B catalysts showed similar tendency.

Acknowledgement

This work was financially supported by the Han project (New Energy Development Project Component and Cell Technology Development for PAFC) through the Korea Institute of Energy Research and by Basic Science Research Institute Project, Ministry of Education, Korea (BSRI 95-314).

References

[1] V.M. Jalan, US Patent 4,202,934 (1980).
[2] T. Itoh, S. Matsuzawa and K. Katoh, US Patent 4,794,054 (1984).
[3] D.A. Landsman and F.J. Luczak, US Patent 4,711,829 (1987).
[4] J.S. Buchanan, G.A. Hards and S.J. Cooper, GB Patent 2,242,203 (1991).
[5] F.J. Luczak, US Patent 5,013,618 (1991).
[6] K. Daube, M. Paffett, S. Gottesfeld and C. Campbell, J. Vac. Sci. Technol. A 4 (1986) 1617.
[7] B.C. Beard and P.N. Ross, J. Electrochem. Soc. 133 (1986) 1839.
[8] B.C. Beard and P.N. Ross, J. Electrochem. Soc. 137 (1990) 3368.
[9] J.S. Chung, K.T. Kim, J.T. Hwang and Y.G. Kim, J. Electrochem. Soc. 140 (1993) 31.
[10] S. Mukerjee and S. Srinivasan, J. Electroanal. Chem. 357 (1993) 201.
[11] B.D. Cullity, *Elements of X-Ray Diffraction,* 2nd Ed. (Addison-Wesley, Reading, 1978) pp. 383–395.
[12] L.J. Cabri, D.R. Owens and J.H. Gilles Laflamme, Canad. Miner. 12 (1973) 21.
[13] M. Shahmiri, S. Murphy and D.J. Vaughau, Miner. Mag. 49 (1985) 547.
[14] H.P. Klug and L.E. Alexander, *X-Ray Diffraction Procedure* (Wiley, New York, 1954).